Multi-Time-Scale Climatic Variations over Eastern China and Implications for the South–North Water Diversion Project

GUOYU REN, HONGBIN LIU, ZIYING CHU, LI ZHANG, XIANG LI, WEIJING LI, YU CHEN, GE GAO, AND YAN ZHANG

Laboratory for Climate Studies, National Climate Center, CMA, Beijing, China

(Manuscript received 2 June 2010, in final form 23 November 2010)

ABSTRACT

Middle and eastern routes of the South–North Water Diversion Project (SNWDP) of China, which are approximately located within the area 28°–42°N and 110°–122°E, are being constructed. This paper investigates the past climatic variations on various time scales using instrumental and proxy data. It is found that annual mean surface air temperature has increased significantly during the past 50–100 years, and winter and spring temperatures in the northern part of the region have undergone the most significant changes. A much more significant increase occurs for annual mean minimum temperature and extreme low temperature than for annual mean maximum temperature and extreme high temperature. No significant trend in annual precipitation is found for the region as a whole for the last 50 and 100 years, although obvious decadal and spatial variation is detectable. A seesaw pattern of annual and summer precipitation variability between the north and the south of the region is evident. Over the last 100 years, the Haihe River basin has witnessed a significant negative trend of annual precipitation, but no similar trend is detected for the Yangtze and Huaihe River basins. Pan evaporation has significantly decreased since the mid-1960s in the region in spite of the fact that the trend appears to have ended in the early 1990s. The negative trend of pan evaporation is very significant in the plain area between the Yangtze and Yellow Rivers. There was a notable series of dry intervals lasting decades in the north of the region. The northern drought of the past 30 years is not the most severe in view of the past 500 years; however, the southern drought during the period from the 1960s to the 1980s may have been unprecedented. The dryness–wetness index (DWI) shows significant oscillations with periodicities of 9.5 and 20 years in the south and 10.5 and 25 years in the north. Longer periodicities in the DWI series include 160–170- and 70–80-yr oscillations in the north, and 100–150-yr oscillations in the south. The observed climate change could have implications for the construction and management of the SNWDP. The official approval and start of the hydro project was catalyzed by the severe multiyear drought of 1997–2003 in the north, and the operation and management of the project in the future will also be influenced by climate change—in particular by precipitation variability. This paper provides a preliminary discussion of the potential implications of observed climate change for the SNWDP.

1. Introduction

The South–North Water Diversion Project (SNWDP) of China is expected to be the largest water diversion project in the world. Two subprojects with eastern and middle routes are already under construction. This hydro project was proposed because north China has experienced frequent droughts, especially since the early 1990s, posing a great challenge to regional economic and social development. Per capita availability of freshwater resources in China is 2200 $m^3\ yr^{-1}$—only a quarter of the world average—and per capita availability of freshwater in the North China Plain is less than 300 $m^3\ yr^{-1}$, which is only 13% of the national average. This is mainly due to the scarcity of precipitation and the large population which accounts for about 45% of the country's total (Academy of Water Resources Planning 2004). When completed, the SNWDP is expected to transfer water at a rate of some 60 billion $m^3\ yr^{-1}$ from the moist Yangtze basin to the semiarid North China Plain, with an objective to mitigate the shortage of water resources in large cities like Beijing and Tianjin.

The SNWDP has raised a series of scientific, social, and environmental concerns related to land use change, climatic change, water pollution control, and agricultural

Corresponding author address: G. Ren, 46 Zhongguancun Nandajie, Haidian District, Beijing 100081, China.
E-mail: guoyoo@cma.gov.cn

DOI: 10.1175/2011JHM1321.1

productivity. Decreases in annual precipitation are considered one of the key causes of the recent successive-year droughts and the significant drop in water availability in north China (Ren et al. 2000; Chen 2002; Fu et al. 2005). As far as climate change is concerned, there are a certain number of scientific questions that need to be answered. For example, what change in climate has occurred over the past 100 years or longer in the areas of the eastern and middle routes of the SNWDP? What can we say about the possible causes for the regional climate change in view of the observational facts? What are the implications of the observed climate changes for the design, construction, and management of the SNWDP?

Research is needed to address these questions and to provide scientific information for water resource managers and decision makers. This work focuses on the first of the aforementioned questions and conducts a series of analyses of observed climate change for the areas of the eastern and middle routes of the SNWDP. However, these analyses also have implications for addressing the other questions raised.

Studies of climate change in eastern China have been conducted for decades (e.g., Zhang and Crowley 1989; Wang and Gong 2000; Ren et al. 2000, 2005; Zhai and Pan 2003; Ge et al. 2003; Liu and Shao 2003; Qian et al. 2004, 2006; Qin et al. 2005; Xu et al. 2006). These studies have generally found large fluctuations of climate on a variety of time scales, and recently it has been confirmed that warming trends of surface air temperature (SAT) exist for areas across the middle and eastern routes of the SNWDP (e.g., Tu et al. 2000; Zeng et al. 2001; Hu et al. 2003; Ren et al. 2005; Ding et al. 2007, 2008). Precipitation and pan evaporation have had different spatial patterns of trends over the past 50 years (e.g., Ren et al. 2000; Ren 2007; Liu et al. 2004; Y. Chen et al. 2005; Xu et al. 2006). The frequency of extreme temperature and precipitation events was also found to change under the background of regional climate warming (e.g., Yan et al. 2002; Zhai and Pan 2003). However, a comprehensive investigation is lacking for the region as a whole and most of the previous analyses in general neither examined regional climate change in relation to water resource management, nor in particular the construction of the SNWDP. In addition, the analyses of instrumental records in the previous studies were mostly based on the datasets up to 1990s, with inhomogeneities of the SAT datasets not examined and adjusted properly (Wang and Gong 2000; Ren et al. 2000; Qian et al. 2004).

Here, we update the dataset of key surface climatic variables to 2004 and provide a comprehensive analysis of the past climatic changes over the eastern and middle route areas of the SNWDP. The SAT data used in the study have been adjusted for inhomogeneities (Li et al. 2004; Ren et al. 2005). Improved processing for the instrumental and proxy data has been made to obtain comparable outcomes with parallel international researches. Following the presentation of the analysis results, including the observed climate change of the past 100 and 500 years, a brief discussion of implications of the research findings for the design, construction, and management of the SNWDP is given, and conclusions are drawn in the final section.

2. Area, data, and methods

The SNWDP consists of three subprojects with eastern and middle routes through the study region. The eastern and middle route (EMR) subprojects are already under construction, and the eastern route will go along the lines of the existing Beijing–Hangzhou Grand Canal flowing through Zhejiang, Jiangsu, Shandong, and Hebei provinces and the municipalities of Tianjin and Beijing (Fig. 1a). Water will be diverted from the Yangtze River within Jiangsu province to Shandong province and Tianjin; the final water volume transferred will reach 26 billion $m^3\ yr^{-1}$. The middle route subproject will construct a new canal from the Dangjiangkou Reserve on the Hanjiang River, a northern tributary of the Yangtze River, to Beijing, flowing through Hubei, Henan, and Hebei provinces and Beijing; the water volume transferred in the first stage of the subproject will be 9.5 billion $m^3\ yr^{-1}$, and it will probably increase to about 13–14 billion $m^3\ yr^{-1}$ in 2050.

We define the study area in two ways. One is to use the natural river catchments, and another is to choose the area defined by 28°–42°N, 110°–122°E for convenience of statistical analysis of the meteorological data (Fig. 1). This region is hereafter referred to as eastern China (EC) for short. It encompasses the Haihe, lower Yellow, Huaihe, and lower Yangtze River basins, including the most densely populated provinces of the country.

Monthly climate data was obtained from the Climate Data Center (CDC) of the National Meteorological Information Center, China Meteorological Administration (CMA). The dataset consists of a total of 740 surface stations across the whole country for the past 50 years. These stations are called national reference climate stations and basic weather stations ("national stations" hereafter). Relatively fewer observational sites are available in the early 1950s. The number of stations in 1951 accounts for only one-fifth of the total, for example, and the network rapidly expanded to 60% and 90% of the total by 1956 and 1960, respectively. The number of stations remains more or less stable after 1960. Observations

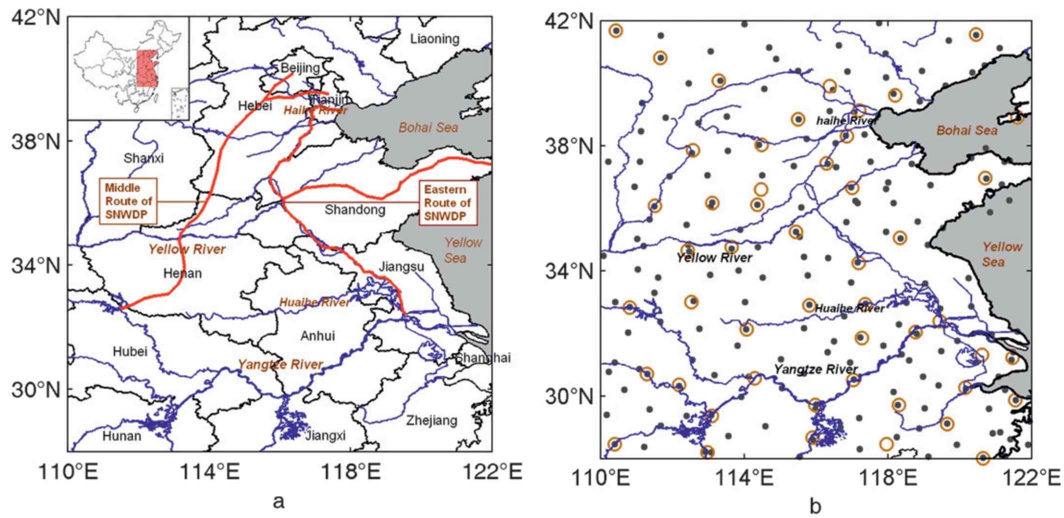

FIG. 1. (a) Study region and (b) distribution of meteorological stations and proxy data sites used in the study. In (a), red lines denote the eastern and middle routes of the SNWDP and the pink color in the insert map indicates the study region within China. Solid small circles in (b) denote locations of the meteorological stations, and large open circles denote proxy data sites.

in the early twentieth century are scarcer; and because of the war, records are mostly nonexistent for a few years during 1941–48.

Inhomogeneities of the monthly mean SAT data during 1951–2004 have been examined and adjusted (Li et al. 2004; Feng et al. 2004; Ren et al. 2005) using the procedure of Easterling et al. (1996), and quality control of other climate variables (precipitation and pan evaporation) has also been made by the CDC–CMA. Within the study region, 193 national stations are chosen for analysis (Fig. 1). The distribution of the stations is relatively uniform across the study region. For a detailed description of the dataset, readers are referred to Li et al. (2004), Ren et al. (2005), and Ren (2007).

In analyzing the climate change for the past century, we also use data from the national stations; but the density of these stations is much sparser in the early twentieth century. We set 1905 as the starting year for the analysis of SAT and precipitation series. We recognize that changes occur in station locations, instruments and instrumental shelters, observation times, and statistical methods for constructing monthly averages for the records of the early twentieth century, which can lead to inhomogeneities in the SAT series. We use the maximum temperature (Tmax) and minimum temperature (Tmin) records rather than the basic four-times-daily records stipulated for post-1950 observations by the CMA, to calculate the monthly mean temperatures throughout the 100-yr temperature series. This to some extent avoids the inhomogeneities of SAT caused by the varied observation times and local time systems used for the pre-1950 period. A previous investigation (Tang and Ren 2005) shows that the Tmax and Tmin measurements are to a large extent independent of the temporal changes of observation times and local time systems that had caused significant discontinuities in daily mean SAT data. However, this statistical method cannot eliminate the inhomogeneities possibly caused by relocations of stations and instrumentation during the earlier period. The processing of the early twentieth century SAT data was explained in detail in Tang and Ren (2005). The 100-yr precipitation data are taken from Wang et al. (2000, 2005).

Regional average surface climate anomaly series are obtained by using the area-weighted method (Jones and Hulme 1996). The EC region is first divided into grids according to longitude and latitude. For this study, longitude–latitude grid boxes of 2.5° × 2.5° size for the most recent 50 years and of 5° × 5° size for the most recent 100 years are used. An arithmetic average is first made of the climate variables and/or their anomalies for all stations within a grid box, and the area-weighted average for all grid boxes in the region or subregions is calculated to obtain the regional average climate time series. SAT and precipitation anomalies are calculated with 1971–2000 as the reference period as recommended by the World Metrological Administration (WMO).

Regional average annual and seasonal (winter, spring, summer, and autumn) mean SAT anomalies series and annual precipitation series for time periods 1956–2004 and 1905–2004 are constructed, and pan evaporation series for time period 1956–2000 are also obtained. The pan

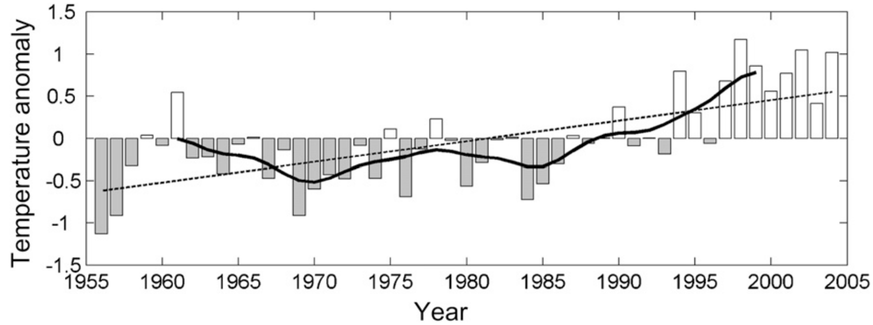

FIG. 2. Change in regional average annual mean temperature anomalies (°C) over the EC region from 1956 to 2004. The dashed line indicates linear trends and the curved line indicates the 11-yr Gaussian smoothed series.

evaporation can be taken as an alternative measurement for potential evaporation. The pans in China were gradually changed to a 600-mm-diameter design from a 200-mm-diameter design after 2000, and 2000 is therefore chosen as the end year to avoid the discontinuities due to the instrumental change. We define the period from December of the previous year to February of the present year (DJF) as winter, March to May (MAM) as spring, June to August (JJA) as summer, and September to November (SON) as autumn. The annual mean is the arithmetic average of the monthly mean values from January to December.

The analysis of the temporal change in dryness–wetness for the past 500 years applies the data derived from ''Yearly charts of dryness–wetness in China over the last 500 years'' (CMA 1982). This dataset was the achievement of a nationwide cooperative effort in the 1970s to collect and synthesize the large quantity of ancient climate information from historical documents for the period 1470–1979, and it has since then been widely used for analyzing the long-term wetness or precipitation change in the country (e.g., Zhang and Crowley 1989; Wang et al. 2005). The 500-yr dryness–wetness series from 120 stations were displayed in the form of isohumes in the atlas (CMA 1982). A five-category scale is used to define the dryness–wetness index (DWI) in the rainy season of May–September. The five categories are denoted qualitatively by the numbers 1, 2, 3, 4, and 5, which respectively represent climate conditions of very wet, wet, normal, dry, and very dry (CMA 1982; Zhang 1988; Zhang and Crowley 1989). The percentages of categories 1, 2, 3, 4, and 5 are about 10%, 20%–30%, 30%, 20%–30%, and 10%, respectively, and thus category 1 (5) is defined as the precipitation more (less) than the sum (difference) of the mean precipitation of May–September and 1.17 times standard deviation for the reference period 1951–80, category 2 (4) as the precipitation more (less) than the sum (difference) of mean precipitation and 0.33 times standard deviation, and category 3 as the precipitation in between, or the precipitation less than the sum of mean precipitation and 0.33 times standard deviation, but more than the difference of mean precipitation and 0.33 times standard deviation (Zhang 1988; Qian et al. 2003). For the most recent 50 years, when the more dense instrumental observations are available, the DWI is calculated directly from the observed rainfall for the months May–September (Zhang et al. 2003).

We use a grid dataset of DWI over eastern China (25°–40°N, 106.5°–121.5°E) with a spatial resolution of 0.5° × 0.5° constructed for other purposes. The dataset covers the rainy season for the period 1470–2000. The observational data from the national reference climate stations over the time period 1951–2000 are used for comparison with the statistical characteristics of the grid DWI data. The kriging method is chosen for interpolating the data (von Storch and Zwiers 1999). Extended

TABLE 1. Trends in mean surface air temperature change in the EC region for 1956–2004 [°C (10 yr)$^{-1}$].

		Annual	Spring	Summer	Autumn	Winter
Trends of temperature change	Mean	0.24**	0.28**	0.03	0.20**	0.43**
	Maximum	0.18**	0.23**	−0.03	0.15*	0.31**
	Minimum	0.31**	0.33**	0.11*	0.25**	0.53**
	Extreme high	0.01	0.01	−0.00	0.03**	0.02
	Extreme low	0.72**	0.50**	0.06	0.50**	0.52**

* Trends that are statistically significant at better than the 5% confidence level by Student's *t* test.
** Trends that are statistically significant at better than the 1% confidence level by Student's *t* test.

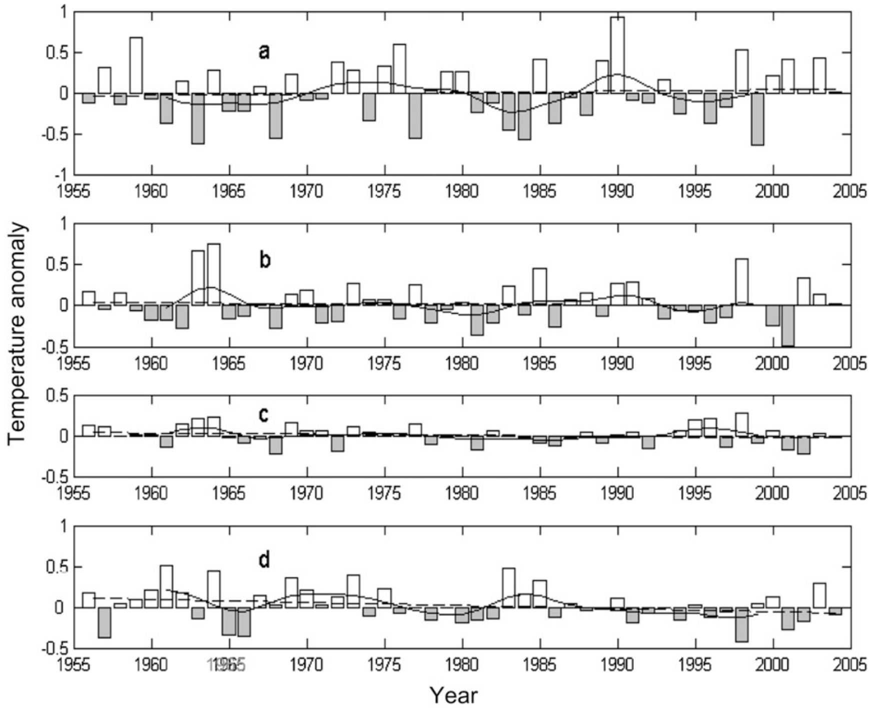

FIG. 3. Change in regional average seasonal mean temperature anomalies (°C) over the EC region from 1956 to 2004. The dashed line indicates linear trend and the curved line indicates the 11-yr Gaussian smoothed series for (a) winter, (b) spring, (c) summer, and (d) autumn.

orthogonal function (EOF) analysis (Torrence and Compo 1998; Hannachi 2004) shows two dominant modes in the data series, with the first mode describing variability over the whole region, and the second showing opposite-signed variability for the north and south, with the main branch of the Huaihe River serving approximately as the dividing line. This result is taken as a basis for dividing the study region into north and south subregions for analysis of the DWI.

The magnitude and direction of climatic trends over the past 100 years (and/or the past 50 years) can be indicated by various metrics, such as rates of change, tendency coefficients, and the difference between the average values of two equal-length subperiods. Rates of change are obtained by using the least squares method to calculate the linear regression coefficients between any climatic variables (e.g., temperature and precipitation) and ordinal numbers of time (e.g., $i = 1, 2, 3...49$ for 1956–2004). Tendency coefficients are defined as the correlation coefficients of any climatic variables (e.g., temperature and precipitation) against ordinal numbers of time. Positive (negative) values of tendency coefficients indicate positive (negative) trends of a climatic variable with time. The significance of the linear trends of the climatic variable is judged by using a t test, except for annual and seasonal precipitation trends, which are estimated by using the rank-based nonparametric Mann–Kendall test (Kendall 1975; Zheng et al. 2007).

EOF analysis (Torrence and Compo 1998; Hannachi 2004) is also applied to the 100-yr annual precipitation data series to identify the leading modes of low-frequency variability in the EC region. Mexican-hat wavelet transforms are employed using the method of Torrence and Compo (1998) to investigate the time and frequency features separately for each of the 100-yr precipitation and the 500-yr DWI data series. Spectral characteristics of the 500-yr DWI series over the south and north subregions of the EC region are also investigated using the singular spectrum analysis (SSA) method (von Storch and Zwiers 1999) in addition to the wavelet transform. Like wavelet transforms, SSA can also indicate how the frequencies and patterns of a time series fluctuate, while power spectral analysis can only be used to examine the frequency feature of a time series.

3. Climate change over the past 100 years

a. 1956–2004

1) TEMPERATURE

Seasonal and annual mean temperatures, maximum and minimum temperatures, and extreme high and low

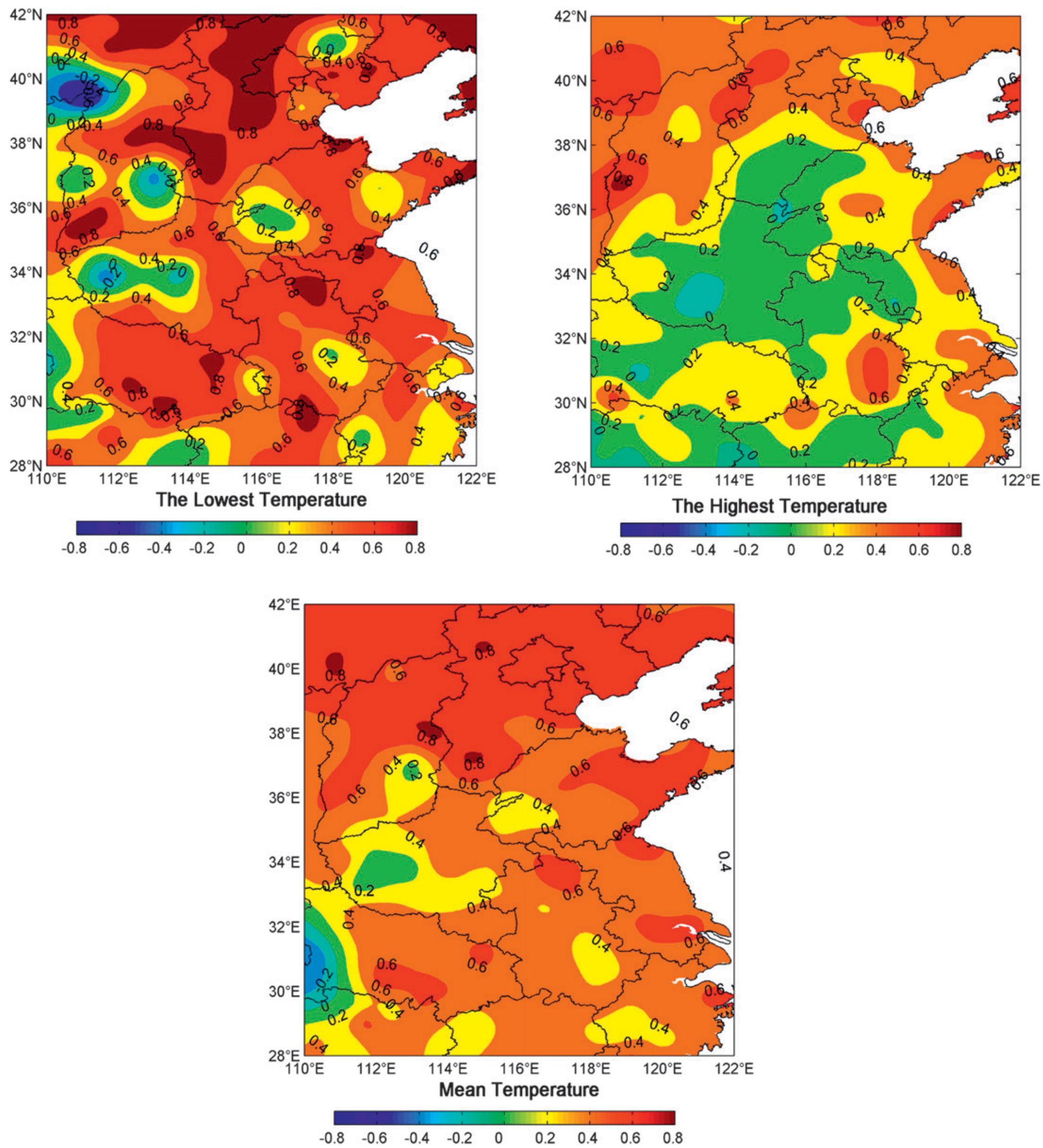

FIG. 4. Trends of annual mean temperatures (°C) over the EC region from 1956 to 2004: (top left) annual mean minimum temperature and (top right) annual maximum temperature. (bottom) Annual mean temperature.

temperatures are examined. The extreme high and low temperatures are the highest and lowest SAT records within a year or a season. The analysis includes both the area-averaged temporal series and the spatial distribution of temperature trends. In the study region, annual mean temperature (AMT) increases significantly during the past 50 years (Fig. 2; Table 1). The linear trend is 0.24°C $(10\ \mathrm{yr})^{-1}$, and the overall warming for the time period is 1.18°C. For comparison, the country-average AMT increases 1.30°C during the same period (Ren 2007). Seasonal mean temperature rises by 0.28°, 0.03°, 0.20°, and 0.43°C $(10\ \mathrm{yr})^{-1}$, respectively, for spring, summer, autumn, and winter, with the largest warming occurring in winter and the smallest in summer (Table 1; Fig. 3). The increase in summer mean temperature is insignificant, and there are even decreases at some sites in the Yangtze–Huaihe River basins.

Both mean Tmin and Tmax increase, but Tmin generally experiences a more significant rise than Tmax (Table 1). Annual mean Tmin and Tmax increase by 0.18° and 0.31°C $(10\ \mathrm{yr})^{-1}$, respectively. Summer mean Tmax witnesses an insignificant decrease. Annual and seasonal mean extreme high and low temperatures have similar changes to mean Tmax and Tmin, and once again little trends can be observed in summer (Table 1). Since larger increases occur in mean Tmin as compared to mean

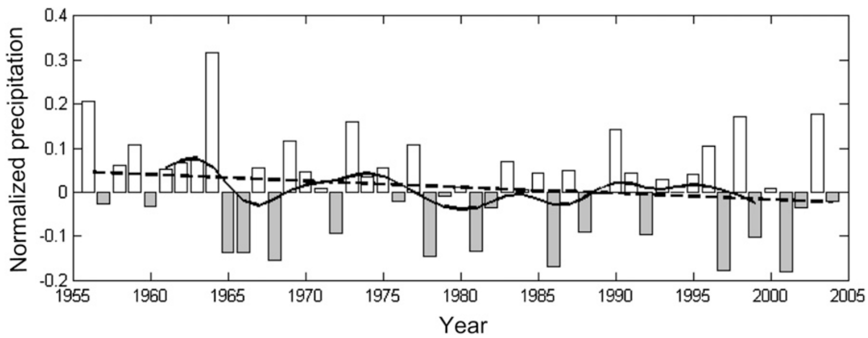

FIG. 5. Percentage change in regional average annual precipitation over the EC region from 1956 to 2004. The dashed line indicates linear trend, and the curved line indicates the 11-yr Gaussian smoothed series.

Tmax, annual and seasonal mean diurnal temperature range (DTR) significantly declines in the EC region.

Figure 4 shows tendency coefficients of AMT and annual mean Tmin and Tmax over the EC region for 1956–2004. The isonephs are drawn automatically by MATLAB, which uses the biharmonic spline interpolation method (Sandwell 1987). The temperature trends are positive for most parts of the region (Fig. 4). AMT north of 36°N undergoes a more significant rise, while some stations in the southwest have a slight cooling trend. The tendency coefficients are generally above 0.5 in the north, indicating that the trends are statistically significant at the 1% confidence level. The largest increase is found for annual mean Tmin, whereas annual mean Tmax generally tends to decrease, especially in the southern part of the region.

2) PRECIPITATION

From 1956 to 2004, an insignificant decrease in the region-averaged annual precipitation occurs, with the highest annual precipitation occurring in 1964, followed by 1956 and 1998 (Fig. 5).

Large regional differences in precipitation trends can be seen in Fig. 6a. In the Yellow and Haihe basins roughly between 34° and 41°N, for example, annual precipitation significantly decreases during the time period analyzed, while the middle and lower reaches of the Yangtze River undergo an obvious rise in annual precipitation. Beijing is located in the drying belt of the north. The linear decrease of annual precipitation in Beijing over the past 50 years is more than 100 mm, or more than 15%. Additionally, annual precipitation over eastern Shandong and southern Liaoning also experience significant negative trends.

Figure 6b shows that the difference between the north and south subregions is mainly caused by the contrasting precipitation trends in summer and winter, while an obvious rise in precipitation in the south, including the Yangtze River basin, is observed. However, the spatial pattern is almost reversed in spring and autumn. It is also clear that the area of rainfall increase around the Yangtze River basin somehow extends to the north in winter, but shrinks to the south in summer. The area north of the Yellow River appears to be rainier in springtime when it is normally very dry as compared to summer and autumn. However, almost all of the seasonal precipitation trends shown in Fig. 6b are statistically insignificant.

Rain days (days with rainfall above 0.1 mm) significantly decrease in the EC region over the past 50 years, with a trend of -5.1 days $(10\ \mathrm{yr})^{-1}$ during the period 1956–2004. On the other hand, days with heavy rain (days with rainfall above 50 mm within 24 h) undergo a slight increase of about $+0.03$ days $(10\ \mathrm{yr})^{-1}$. Spatially, the increase in days with heavy rain mostly occurs in the south. As the total annual precipitation shows no significant trend, the decrease in rain days indicates a generally enhanced intensity of precipitation over the past 50 years. This is consistent with the slightly increased days with heavy rain.

3) PAN EVAPORATION

Figure 7 shows the change in area-averaged annual pan evaporation over the study region. During 1956–2000, the maximum of pan evaporation occurs around 1966. Since then, it has significantly decreased, but the decrease comes to an end in the early 1990s. The temporal change is very similar to that reported by Liu et al. (2004), Ren et al. (2005), Ren (2007), Guo and Ren (2005), and D. Chen et al. (2005). Summer is the time of the greatest drop, but spring and autumn also experience significant decreases (Guo and Ren 2005; Ren 2007). Previous investigations (Guo and Ren 2005; Ren 2007) have analyzed the climatic factors influencing the trends of pan evaporation for the past half century and have found that the decline is related to a significant decrease in sunshine duration–solar radiation, which might have been caused by the rising concentration of aerosols in the atmosphere, and the tremendous drop of

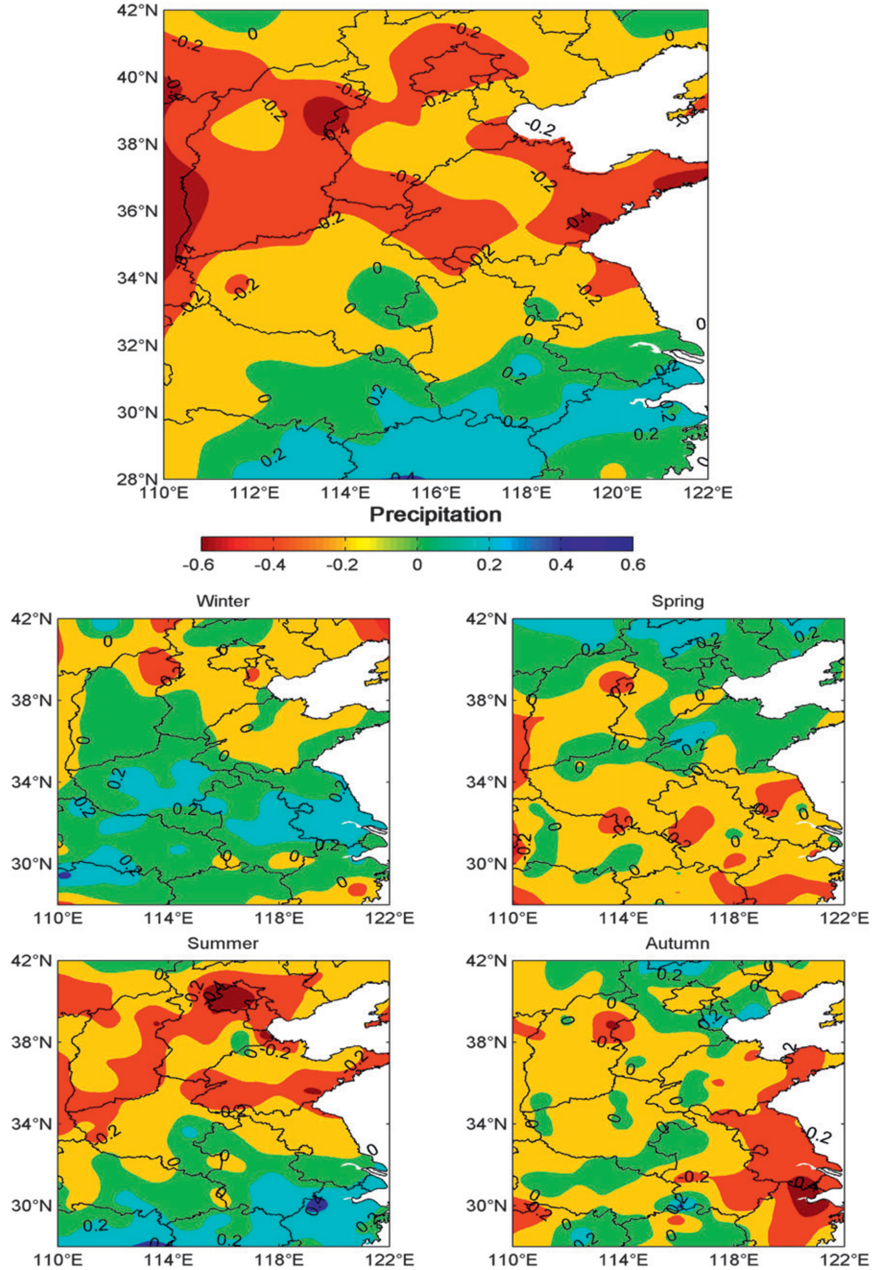

FIG. 6. Spatial distribution of (top) annual and (middle left) winter, (middle right) spring, (bottom left) summer, and (bottom right) autumn precipitation trends over the EC region from 1956 to 2004.

near-surface wind speed observed at most meteorological stations.

The decrease in pan evaporation takes place in most areas, but is most significant between the mid–lower reaches of the Yangtze and Yellow Rivers (figure not shown). There is a narrow belt with a slight rising trend stretching from the westernmost to northernmost areas. The spatial pattern of pan evaporation trends in summer is similar to that for annual pan evaporation, indicating the large contribution of summer pan evaporation changes to the annual trend. In the other seasons the decrease is weaker, and pan evaporation at some stations in the Yangtze basin even slightly increases in spring.

The ratio of pan evaporation and precipitation, which can be taken as an indicator of dryness, shows alternating dry and wet periods in the EC region (figure not shown). For example, 1964 and 1998 are the wettest years, and 1978 is the driest year. Although the regional average

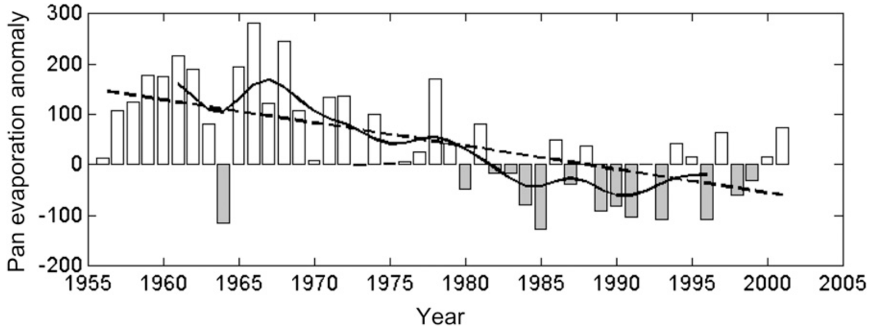

FIG. 7. Change in annual pan evaporation (mm) over the EC region from 1956 to 2000. The dashed line indicates linear trend, and the curved line indicates the 11-yr Gaussian smoothed series.

dryness sees no significant linear trend, the spatial pattern of change in dryness indicates an obvious drying phenomenon in the north and a more significant moistening trend in the south, consistent with the trends of annual or summer precipitation to a large extent.

b. 1905–2004

1) TEMPERATURE

Figure 8 shows annual, winter, and summer mean SAT anomalies for the past 100 years. A general positive trend for AMT is clearly observed, with the 1990s being the warmest decade in the past 100 years. The warmer climate from the mid-1930s to mid-1940s is also obvious. The early-period data sites are relatively sparse, but the cooler climate in the period from the 1900s to the 1910s appears real, since this is also reported in previous analyses using different datasets and methods (e.g., Qian et al. 2004; Tang and Ren 2005). The linear trend of AMT over the past 100 years is 0.07°C $(10\ \mathrm{yr})^{-1}$, which is close to the countrywide average AMT trend (Tang and Ren 2005; Ding et al. 2008) and the global average AMT trend (Jones and Moberg 2003; Houghton et al. 2001; Solomon et al. 2007) for similar time periods.

A larger increase is seen for winter mean SAT, with the trend reaching 0.17°C $(10\ \mathrm{yr})^{-1}$, while summer undergoes cooling during the time period analyzed, especially for the period from the 1940s to the 1980s (Fig. 8). It is also evident that the summers in the period from the 1930s to the 1940s are the warmest on record. These features are very similar to those for the countrywide average seasonal temperature change (Tang and Ren 2005; Ding et al. 2008). It can be inferred that the yearly temperature range in the region had experienced a significant decrease over the past 100 years because of the warming in winter and cooling in summer.

With regard to the interbasin difference, the Haihe and Huaihe basins of the north witness more significant warming than does the Yangtze basin. The 1990s are among the warmest decades for every basin, and the period from the 1930s to the 1940s is the second warmest, especially in the Huaihe basin. The Yangtze basin has a warming trend in annual and seasonal mean SAT except for summer, which experiences a cooling. Although positive anomalies are observed for each season of the 1990s, the values of the anomalies are relatively lower than in the period from the 1930s to the 1940s in the Yangtze basin, especially in summer.

2) PRECIPITATION

The results of the Mann–Kendall test show that there are no significant trends for annual and seasonal precipitation for the last 100 years in the study region (Fig. 9). The normalized annual precipitation anomalies indicate that there is a relatively wet period lasting from the mid-1940s to the early 1960s. A long dry period from the mid-1910s to the mid-1940s can be seen, and the climate is also drier since the late 1990s. The results for the early years should be treated with caution, however, since the number of stations is small for the early years, especially for the pre-1920s period (Fig. 9).

In spite of the fact that the Haihe basin sees no obvious long-term trend over the last 100 years, the annual precipitation of the Huaihe basin shows a slight increasing trend and a larger decadal variation (figures not shown), with low values frequently occurring before the mid-1950s and relatively high values occurring in the period from the mid-1950s to the 1970s. The Yangtze basin has a similar change as the Huaihe basin, with a relatively dry period from the 1920s to the 1940s and a wetter period appearing after the early 1990s.

The annual precipitation for 1905–2004 in the region is further decomposed by EOF analysis. Figure 10 shows the distribution of the first eigenvectors. Positive values can be found in the area south of 35°N, roughly in the Yangtze–Huaihe basins, while negative values appear in the northern area of the middle and lower reaches of the Yellow and Haihe Rivers. The regional discrepancy

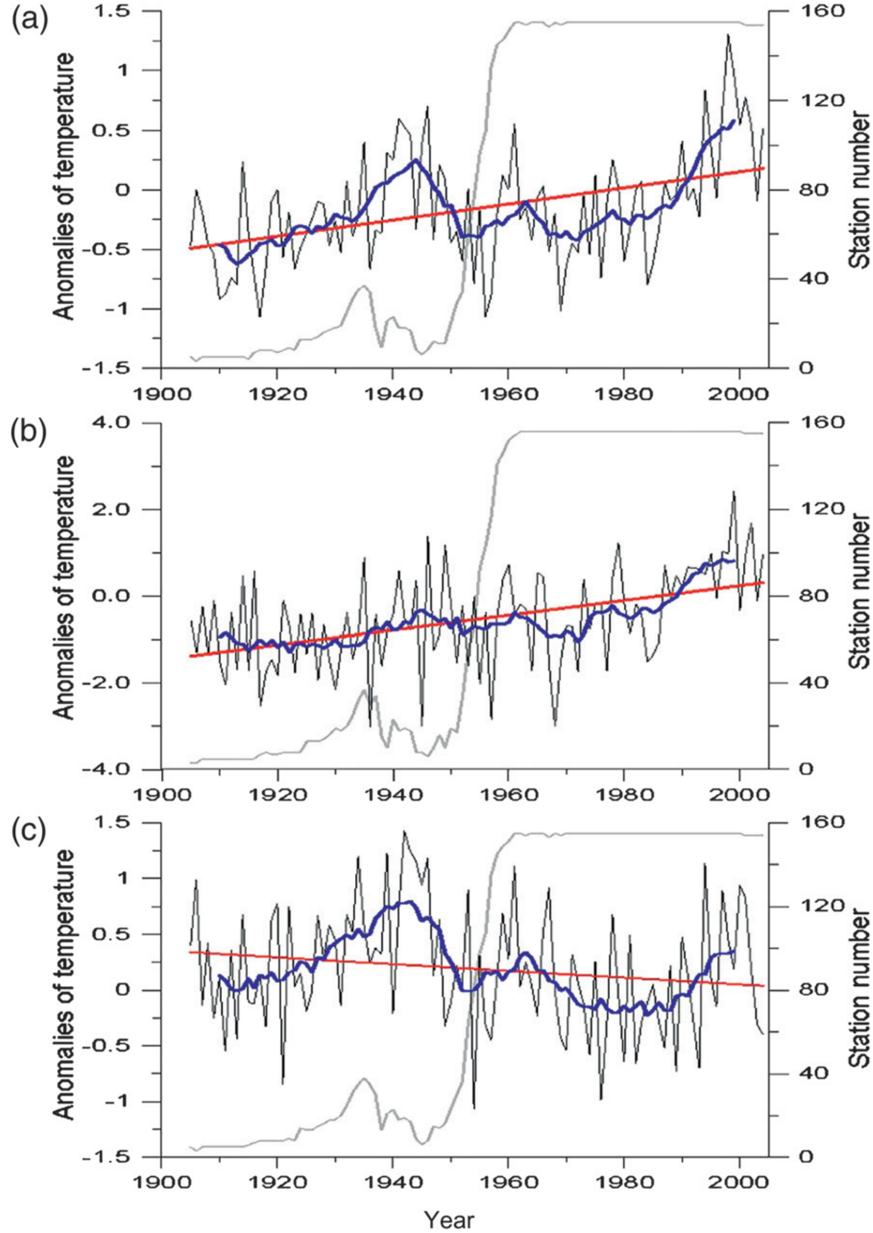

FIG. 8. (a) Annual, (b) winter, and (c) summer mean surface air temperature anomalies (°C) over the EC region during 1905–2004. Black line = temperature anomalies (relative to 1971–2000), bold blue line = 11-yr running average of temperature anomalies, red line = linear trends, and gray line = number of stations.

suggests a spatial pattern with seesaw variability of annual precipitation between the north and the south. When the Yangtze–Huaihe basins are rainy, it is usually drier in the Yellow and Haihe basins. Simple correlation analysis also shows the significant negative relationship between annual precipitation of the Haihe basin and the lower Yangtze basin within the study region for the last 50 years.

Based on the leading EOF's contour of 0.05, which lies approximately along the main branch of the Huaihe River, the study region can be divided into southern and northern portions. Figure 11 shows the respective variations of annual precipitation anomalies in the two areas. It is obvious that there is a relatively dry period from the beginning of the record to the 1940s in the north. The climate then turns rainier after the mid-1940s. A second dry period lasts from the mid-1980s to the present in the north. The multidecadal fluctuations of annual precipitation in the north indicate a roughly 60-yr periodicity.

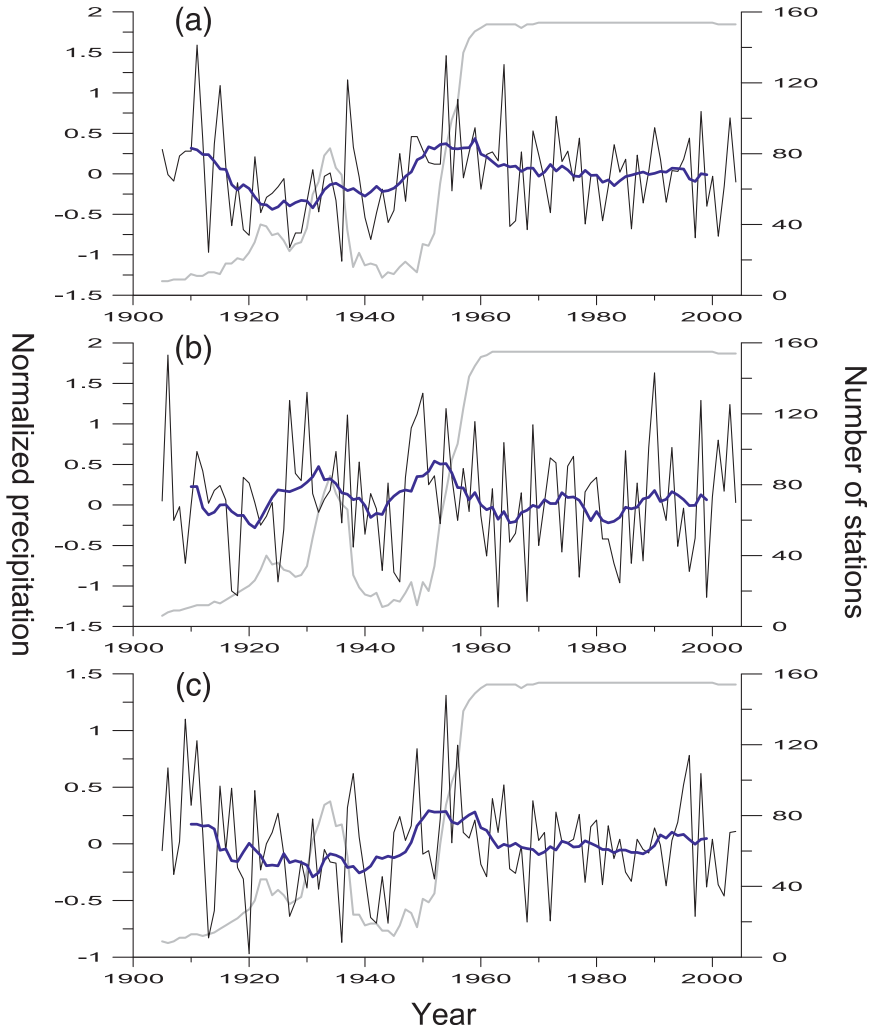

FIG. 9. Normalized (a) annual, (b) winter, and (c) summer precipitation over the EC region during 1905–2004. Black line = normalized precipitation, bold blue line = 11-yr running average, and gray line = number of stations.

Annual precipitation anomalies in the south show more gentle variability during the 100 years (Fig. 11). A severe drought lasted from the beginning of the twentieth century to the mid-1940s, which is consistent with the climatic condition in the north. From the mid-1940s to the early 1980s, however, annual precipitation in the south remains almost unchanged in spite of the larger interannual variability. After the early 1980s, the climate turns more moist again, with the annual precipitation anomalies being mostly positive during the last 20 years. The periodicities in the south are not as clear as in the north, though an approximately 40–50-yr oscillation could be claimed from Fig. 11. A wavelet power spectrum of annual precipitation in the two areas shows statistically significant (at the 5% confidence level) 4-yr periodicity in the north and 16-yr periodicity in the south.

4. Changes in dryness over the past 500 years

Figure 12 shows two representative types of spatial patterns of historical drought and rainy conditions in the EC region. In the summer of 1586, a severe drought occurred in most areas in the north, while a wet climate prevailed in the south. In 1652, on the other hand, a reversed pattern can be seen, with a wet climate prevailing in the north and a dry climate in the south. Previous studies also show that the seesaw variation of drought and floods in the EC region over the past 500 years is one of the dominant modes of interannual and decadal variability (e.g., Wang et al. 2005).

Statistics of the 500-yr drought and flood events show that 31.5% of all years are dry years (DWI > 3) in the north, while only 21.6% of all years are dry years in the

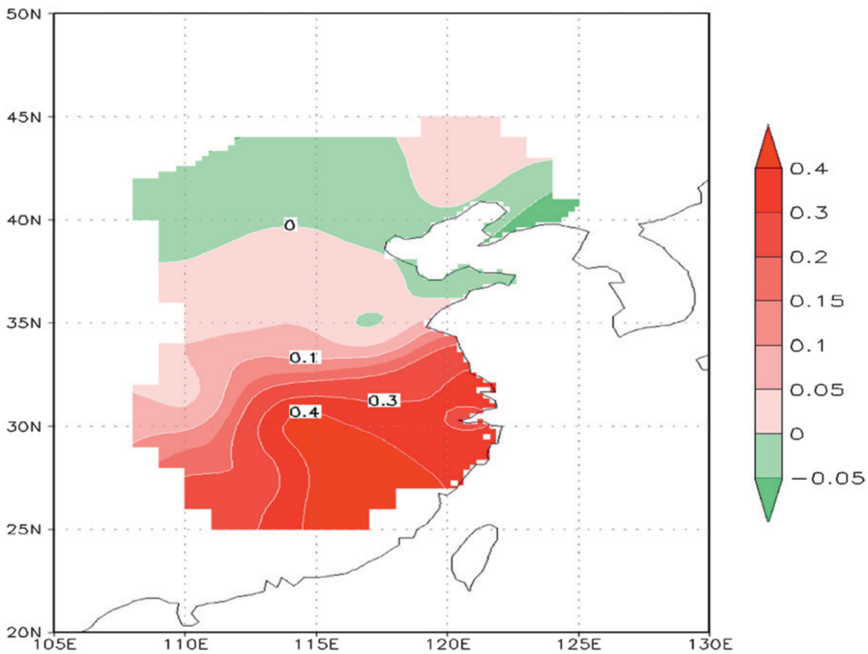

FIG. 10. Leading EOFs for annual precipitation series of the past 100 years in the EC region.

south (Table 2). For the very dry years (DWI = 5), the frequency is only 3.9% in the south but 6.9% in the north. The frequencies of dry years (DWI = 4) are 17.7% and 24.3% in the south and north, respectively. For the wet years (DWI < 3), there are no significant differences between the north and south. Therefore, the north has a generally drier climate and more frequent droughts than the south during the last 500 years.

Figure 13 shows DWI changes in the north and the south, respectively, in the past 500 years. The DWI in the north shows not only larger mean values (drier climate conditions), but larger standard deviations than in the south. More obvious decadal variation in DWI, and therefore more evident dry–wet periods, can be seen in the north. A dry interval occurred from the 1470s to the 1530s in the north, for example, while in the south the climate was near normal during this interval. A long wet interval in the south lasted from the 1830s to the 1950s, but alternating wet and dry stages occurred in the north during this period. It is also worth noting that there were a few time periods that experienced multidecadal droughts similar to the recent two-decade drought in north China. These periods of severe droughts include the late 1480s to the 1490s, the 1520s to the 1530s, and the 1630s to the 1640s, with the severity of the droughts in some years being larger than that of the 1997–2004 north China drought. Although the drought in the north in the past 20 years might not be the most severe in recorded history, the southern drought during the period from the 1960s to the 1980s may be unprecedented.

The wavelet and SSA analyses produce similar results. Figure 14 shows the power spectra and coefficients of the real part of the wavelet analysis. Positive (negative) coefficients correspond to dry (wet) conditions. There are 160–170- and 70–80-yr components in the north; however, the intensity of the two components and their evolution are different, with the 160–170-yr component becoming longer and weaker with time and the 70–80-yr component becoming shorter and stronger with time. For the south, a 100–150-yr periodicity is obvious for the earlier 300 years, but it is gradually overtaken by a quasi-200-yr periodicity during the last two centuries. A 50-yr periodicity during 1500–1700 and an 80-yr periodicity during 1800–2000 are also detectable for the south. Both the north and the south display a 20–25-yr oscillation. The result from the SSA analysis (not shown here) shows longer dominant periodicities in the north than in the south, with significant oscillatory periods of roughly 10.5 and 25 years in the north and 9.5 and 20 years in the south.

Therefore, the multiscale periodicities in the 500-yr DWI series do exist in eastern China. The periodicities on the decadal scale are partly supported by the analyses of instrumental records of the past 100 years. Generally speaking, the DWI in the north shows longer and stronger oscillations than those in the south.

Signals of climatic shifts in the DWI series for the north and south areas are also examined using t, F, and Lepage

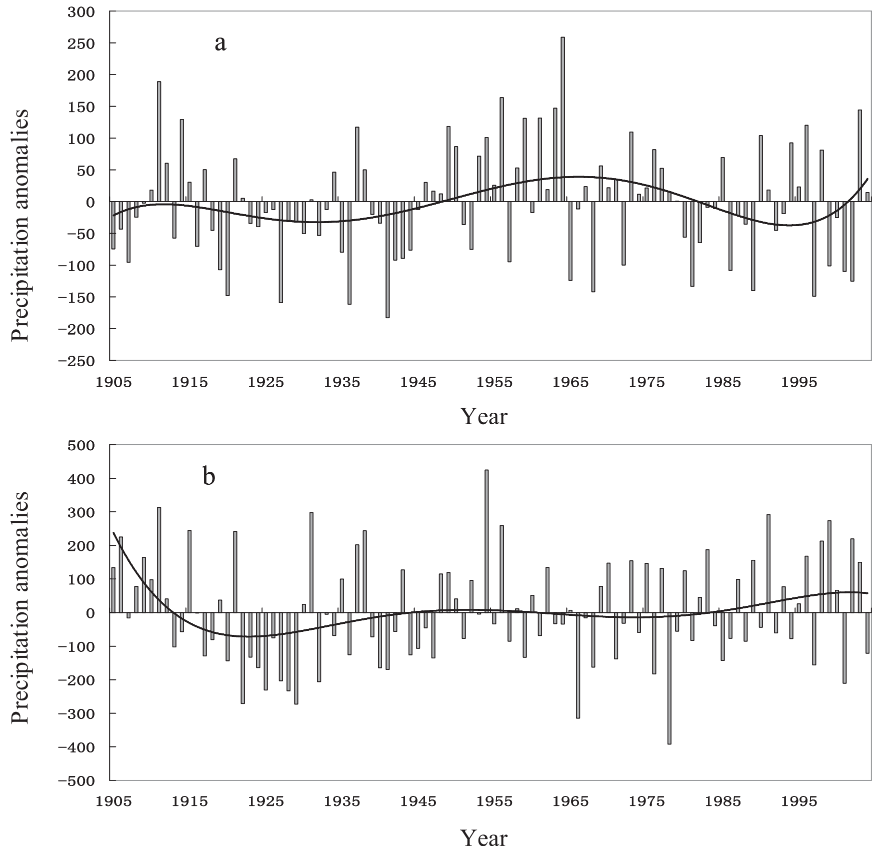

FIG. 11. Annual mean precipitation anomalies (mm) in (a) the north and (b) the south of the EC region from 1905 to 2004. The curves are a fifth-order polynomial regression fit to the data.

tests. All methods demonstrate the abrupt change from a drier climate to wetter conditions during the time period 1643–50 in the north. For the south, climatic shifts are also detectable in the same time period, but the signal is relatively weaker. During the last 250 years, there is no significant climatic shift for either the north or the south.

5. Discussion

a. *Causes of climate change*

Although it is still premature to answer the question of what has caused the observed changes in climate in the EC region, our analysis is favorable to an explanation by natural causes for the annual and summer precipitation. The data series of both the past 100 and 500 years show decadal to multidecadal variations. The much-below-normal precipitation and the severe drought of the last two decades in the north are not unprecedented in view of the 500-yr DWI series, implying that these events may have occurred naturally. Other researchers share similar points of view based on their investigations of precipitation variability in eastern China (e.g., Wang et al. 2000; Li and Xian 2003; Ding and Sun 2003), and some relate the summer precipitation variability to the decadal shifts of the eastern Asian monsoon (Wang 2001; Zhou and Huang 2003; Ding and Sun 2003; Ding et al. 2008).

Our analysis indicates a significant warming in the EC region for both the past 50 and 100 years. The temporal and spatial characteristics of the warming are similar to those of global land SAT change, probably suggesting a uniform forcing of the increased concentration of greenhouse gases in the atmosphere (Houghton et al. 2001; Solomon et al. 2007). Studies in China also support the claim that the warming in eastern China is likely caused by the anthropogenic increase in atmospheric CO_2 concentration (Qin et al. 2005; Zhao et al. 2005; Ding et al. 2007, 2008). It should be noted, however, that the urbanization effect on SAT change has not been removed from the warming trend given in this paper. Previous studies find significant effects of urbanization on the recent trends of SAT for single stations and regionally averaged temperature series in China (Ren et al. 2005, 2008). Taking the urbanization effect into account, the regional warming trend will be largely weakened, though it will be still significant.

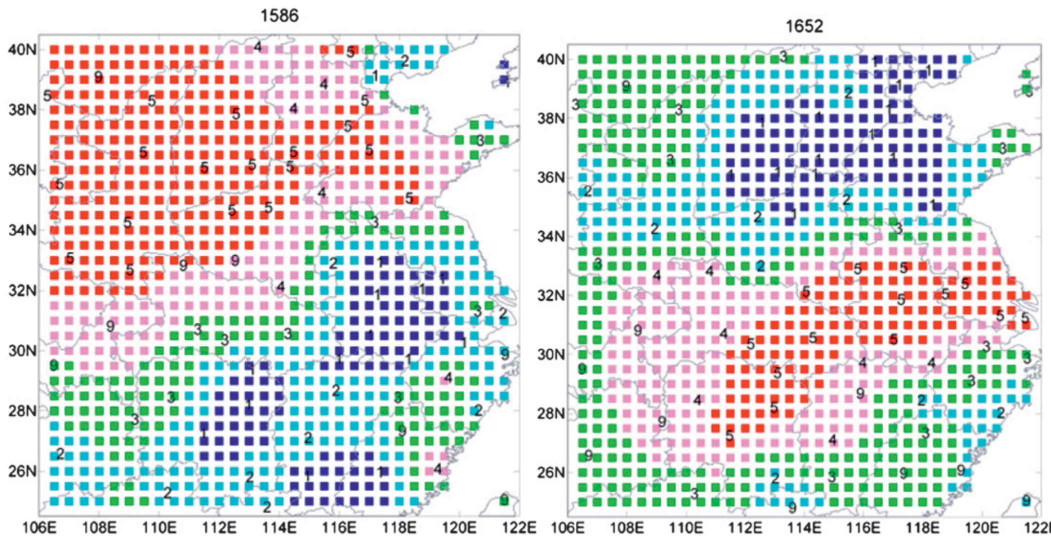

FIG. 12. Two types of dryness–wetness distribution patterns in summer in EC [(left) year 1586 and (right) year 1652]. The numbers show the location and DWI of each site and the colored squares show the DWI for each grid point: 1 and purple = very wet, 2 and blue = wet, 3 and green = normal, 4 and pink = dry, 5 and red = very dry, and 9 = missing data.

b. Climate background of the SNWDP

Large climate change and variability have occurred in the study region. These include the significant warming in annual and cold season mean SAT during the past 50 and 100 years and the significant negative trend in annual and summer precipitation in the north during the same time periods, with 1997–2004 being the driest interval of the past 50 years. The obvious trend toward drier conditions has played a key role in the deteriorating water supplies of the north in the past two decades, during which water demand has significantly increased. In particular, the severe drought of 1997–2004 in the north has facilitated the water shortages in the Haihe basin. Although the SNWDP had been under evaluation since the 1950s, the EMR subprojects were only finally approved by the central government around 2000, when the water availability in the north was already at its lowest level of these several decades because of the severe drought during the transition of the centuries.

The concern is that, if the long-term drying trend and the 1997–2004 drought were caused by natural variability (e.g., Huang and Zhou 2002; Ren 2007) rather than by anthropogenic influence on atmospheric compositions and regional land cover, then precipitation in the northern part of the EC region will recover sooner or later to normal levels or even higher, implying that a moistening trend in the coming decades is possible. The multidecadal or periodic features of annual and summer precipitation in the north have been confirmed. Aerosol emissions due to human activities are considered to be another possible factor for the observed decrease in precipitation in north China (e.g., Xu 2001; Menon et al. 2002). The emission of pollutants, however, will probably be reduced because of the increasing concerns over local environmental quality, and the impact of aerosols on precipitation, if any, will be weakened in the future.

This is not to imply that the decision to launch the SNWDP has been incorrect. Decisions of such magnitude should be made on the basis of a balanced consideration of complex factors. Population growth and rising water consumption are important factors. However, considerable attention should be given to the climatic background in assessing the approval and launch of such hydrological projects. If the reference years were chosen to cover a longer time period, the calculation of the water availability and water balance would be different. In any condition, the possible recovery or increase of precipitation in the coming decades will significantly affect the water availability and water demands of the Haihe basin, which will in turn affect

TABLE 2. Percentages of dry–wet years in the EC region over the past 500 years (DWI categories: 1 = very wet, 2 = wet, 3 = normal, 4 = dry, and 5 = very dry).

DWI	1	2	3	4	5
North	5.67	22.70	40.37	24.34	6.92
	28.37			31.26	
South	5.01	24.56	48.84	17.69	3.90
	29.57			21.59	
Whole region	5.34	23.63	44.61	21.01	5.41
	28.97			26.42	

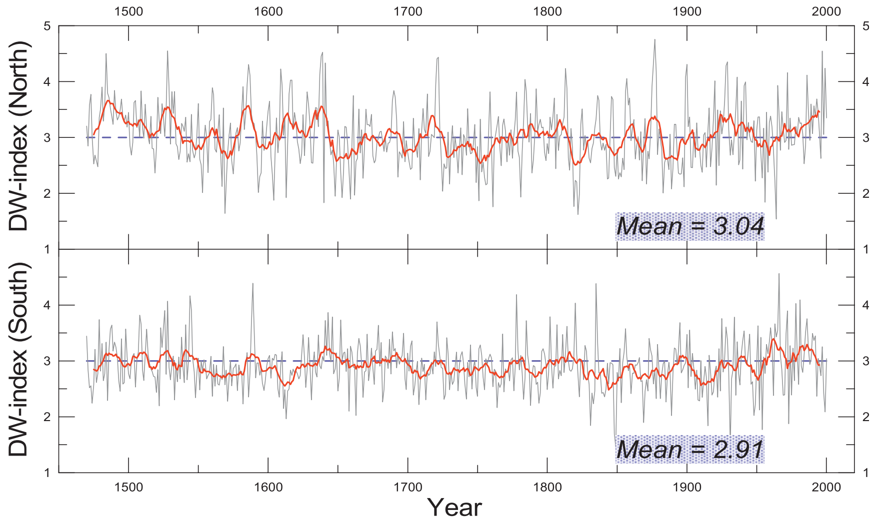

FIG. 13. DWI changes in the (top) north and (bottom) south parts of the EC region over the past 500 years (1470–2000). Red line = 11-yr Gaussian smoothed series; DWI categories: 1 = very wet, 2 = wet, 3 = normal, 4 = dry, and 5 = very dry.

the water volume needed to be diverted from the Yangtze River to the north. Therefore, the future operation and management of the SNWDP should be based on robust scientific information of climate variability.

c. Spatial pattern of precipitation variation

A seesaw pattern of annual and summer precipitation variability between the north and the south is detected for varied time scales. The spatial pattern is characterized by a higher possibility of the simultaneous occurrence of droughts (wet spells) in the north and wet spells (droughts) in the south. This implies that, when summer precipitation is less than normal and water availability falls in the north, there is a higher possibility that water will be available in the lower Yangtze River for being transferred to the north. Similarly, when summer precipitation is more than normal in the north and there is less need for transferring water from the south, the precipitation and discharge of the lower Yangtze River will be more likely below normal. Without regard to the issues of water pollution, the seesaw pattern of precipitation variability lends support to the feasibility of the eastern route subproject of the SNWDP.

We also find a few time periods with multidecadal droughts in the historical DWI series, similar to the recent two-decade drought in the north, and these include the droughts of the late 1480s to the 1490s, 1520s to the 1530s, and the 1630s to the 1640s. The severity of some of the ancient droughts is larger than that of the recent droughts. The findings are confirmed by the previous studies (e.g., Zhang and Crowley 1989; Wang et al. 2005; Zheng et al. 2006). The multidecadal mega-droughts in history and the possibility of the occurrence of more severe than present droughts lends more support to the construction of the EMR subprojects of the SNWDP, especially when considering the increasing population and water demands in decades to come.

It is worth noting that the drought occurrences of varied durations and magnitudes are telling different stories, and they imply alternative recommendations of adaptation options for policymakers. The construction and operation of the SNWDP should be based on the full spectrum of scientific and social–economic information.

6. Conclusions

1) In the study region, AMT increases significantly during 1956–2004 at a rate of 0.24°C $(10\ \mathrm{yr})^{-1}$. Winter and spring undergo the largest warming and summer witnesses an insignificant trend, with the Yangtze–Huaihe basins even experiencing a slight cooling. The increase in annual mean minimum temperature is considerably higher than the increase in annual mean maximum temperature, while the increase in annual extreme low temperature is 10 times that of the annual extreme high temperature. As a result, annual mean DTR and yearly temperature range are declining. AMT in the north undergoes a more significant increase than in the south.
2) No significant trend in annual precipitation is found for the past 50 years, but the study region has the highest precipitation in the 1950s and below-normal precipitation in the 1960s, 1970s, and 1980s. The climate is becoming drier in the Yellow and Haihe basins, while the middle and lower reaches of the Yangtze River

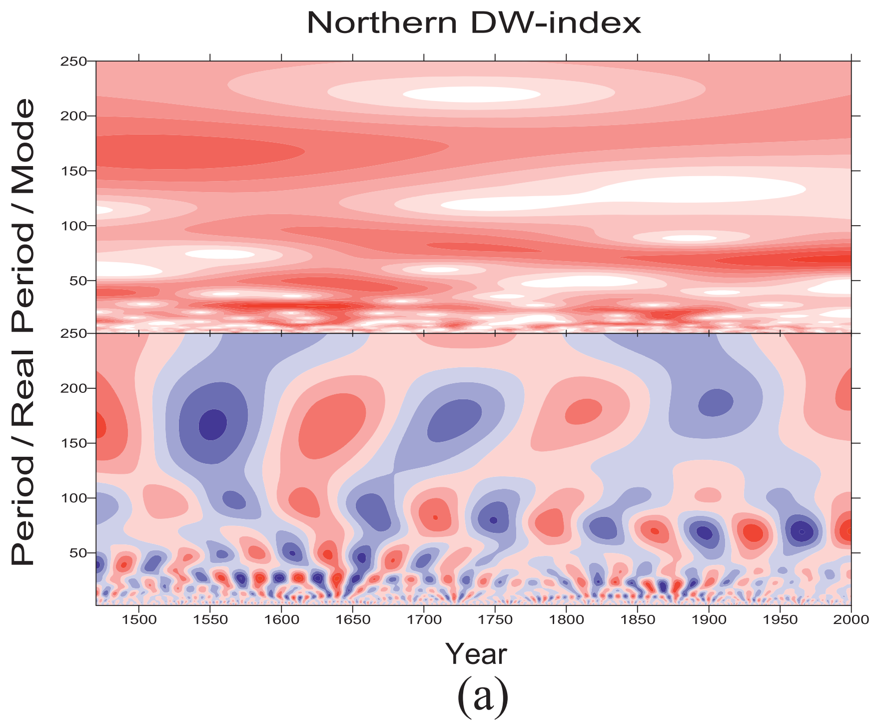

FIG. 14. Wavelet analysis results of the 500-yr DWI series over the EC region: (a) north and (b) south.

are undergoing a moistening trend. The increase in precipitation in the south mainly occurs in summer and winter. Days with rain generally decrease over the 50-yr period, but days with heavy rain have a slight rising trend, implying an increase in the intensity of precipitation.

3) Pan evaporation has significantly decreased in the study region since the mid-1960s, but the decrease

comes to an end in the early 1990s, despite the fact that the long-term trend over the whole time period is still negative. The largest drop in pan evaporation occurs in summer between the Yangtze and Yellow Rivers. The ratio of pan evaporation and precipitation shows little change in the region as whole.

4) A general positive trend of AMT is also obvious for the past 100 years, with the linear trend reaching 0.08°C $(10\ \text{yr})^{-1}$. Warmer climate prevails in the time periods from the 1930s to the 1940s and the 1980s to 2004. A larger warming is seen for winter, while summer undergoes an insignificant cooling.
5) No significant trend is found for the regional annual and seasonal precipitation during 1905–2004. However, there is a relatively wet period lasting from the mid-1940s to the early 1960s, and there is also a long dry period from the mid-1910s to the mid-1940s. The Haihe basin experiences an obvious decline in annual precipitation over the 100-yr period, but no detectable trend is found for the Yangtze and Huaihe basins. Relatively dry periods in the north are found in the earliest 40 years and the latest 30 years.
6) A spatial pattern showing a seesaw of variability in annual precipitation between the north and the south is identified in the 100-yr precipitation series, indicating that the wetter (drier) years in the Yangtze–Huaihe basins are usually accompanied by drier (wetter) conditions in the Yellow and Haihe basins. The multidecadal fluctuation of precipitation indicates a roughly 60-yr periodicity in the north and 40-yr periodicity in the south.
7) The seesaw of decadal DWI variations between the north and the south also exists over the past 500 years. More obvious decadal variations of DWI occur in the north. A series of dry intervals lasting for decades in the north is evident. The northern drought of the most recent 30 years is not the most severe event in view of the historical record, but the drought in the south in the period from the 1960s to the 1980s may be unprecedented.
8) DWI in the north has longer dominant periodicities than in the south. Significant periodicities in the south occur at 9.5 and 20 years, while 10.5- and 25-yr periodicities are more significant in the north. However, the signal of the 25-yr oscillation in the north has become weaker over the last two centuries, and the 9.5-yr oscillation in the south is weak in the first two centuries of the past 500 years. The wavelet analysis also reveals 160–170- and 70–80-yr components of variability in the north, and 100–150-yr oscillations in the south.
9) Our analysis indicates the dominance of natural variability in the annual and summer precipitation of eastern China for the time scales concerned, although the large warming of the last 50 years may have been partly affected by the anthropogenic increase in atmospheric CO_2 concentration. Regardless of causes, the observed change in annual and summer precipitation has affected the water cycle and water resources over the EMR areas of the SNWDP. The precipitation change is not only the catalyst for the launch of the SNWDP, but will continue to be a key influential factor for the management and operation of the water diversion project in the future.

Acknowledgments. The study is supported by the Italian Ministry for the Environment and Territory (IMET) under the Sustainable Water Integrated Management of the East Route (SWIMER) in the South–North Transfer Project, the Ministry of Science and Technology of China (Project 2007BAC29B02), and the Ministry of Water Resources of China (Project 200801001).

REFERENCES

Academy of Water Resources Planning, 2004: The national water resources assessment: A component of the national integrated planning of water resources. Academy of Water Resources Planning, 230 pp.

Chen, D., G. Gao, C.-Y. Xu, J. Guo, and G. Ren, 2005: Comparison of Thornthwaite method and pan data with the standard Penman-Monteith estimates of reference evapotranspiration for China. *Climate Res.,* **28,** 123–132.

Chen, Y., G. Gao, and G. Ren, 2005: Spatial and temporal variation of precipitation over ten major basins in China between 1956 and 2000. *J. Nat. Resour.,* **20,** 637–643.

Chen, Z., 2002: Consecutive drought and water crisis in north China. *China Water Conservancy,* **466** (4), 8–12.

CMA, 1982: *Yearly Charts of Dryness/Wetness in China over the Last 500 Years*. China Meteorological Press, 530 pp.

Ding, Y., and Y. Sun, 2003: Interdecadal variability of the precipitation patterns in the east-Asian monsoon region. *Climate Change Newsletter,* China IPCC Office and National Climate Center, Beijing, China, 22–24.

——, G. Ren, Z. Zhao, Y. Xu, Y. Luo, Q. Li, and J. Zhang, 2007: Detection, causes and projection of climate change over China: An overview of recent progress. *Adv. Atmos. Sci.,* **24,** 954–971.

——, Z. Wang, and Y. Sun, 2008: Inter-decadal variation of the summer precipitation in east China and its association with decreasing Asian summer monsoon. Part I: Observed evidences. *Int. J. Climatol.,* **28,** 1139–1161.

Easterling, D. R., T. C. Peterson, and T. R. Karl, 1996: On the development and use of homogenized climate datasets. *J. Climate,* **9,** 1429–1434.

Feng, S., Q. Hu, and W. H. Qian, 2004: Quality control of daily meteorological data in China, 1951–2000: A new dataset. *Int. J. Climatol.,* **24,** 853–870.

Fu, C., Z. An, and W. Guo, 2005: Evolution of life-supporting environment in our nation and the predictive study of aridification in northern China. I. Main scientific issues and achievements. *Adv. Earth Sci.,* **20,** 1168–1175.

Ge, Q.-S., J. Zheng, X. Fang, Z. Man, X. Zhang, P. Zhang, and W.-C. Wang, 2003: Winter half-year temperature reconstruction for the middle and lower reaches of the Yellow River and

Yangtze River, China, during the past 2000 years. *Holocene,* **13,** 995–1002.

Guo, J., and G. Ren, 2005: Recent change of pan evaporation and possible climate factors over the Huang–Huai–Hai watershed, China. *Adv. Water Sci.,* **16,** 666–672.

Hannachi, A., 2004: A primer for EOF analysis of climate data. University of Reading, 33 pp.

Houghton, J. T., Y. Ding, D. J. Griggs, M. Noguer, P. J. van der Linden, X. Dai, K. Maskell, and C. A. Johnson, Eds., 2001: *Climate Change 2001: The Scientific Basis*. Cambridge University Press, 881 pp.

Hu, Z.-Z., S. Yang, and R. Wu, 2003: Long-term climate variations in China and global warming signals. *J. Geophys. Res.,* **108,** 4614, doi:10.1029/2003JD003651.

Huang, R., and L. Zhou, 2002: Characteristics, forming mechanism and prediction research of major meteorological disaster. *J. Nat. Disaster,* **11,** 1–9.

Jones, P. D., and M. Hulme, 1996: Calculating regional climatic time series for temperature and precipitation: Methods and illustrations. *Int. J. Climatol.,* **16,** 361–377.

——, and A. Moberg, 2003: Hemispheric and large-scale surface air temperature variations: An extensive revision and an update to 2001. *J. Climate,* **16,** 206–223.

Kendall, M. G., 1975: *Rank Correlation Measures*. Charles Griffin, 202 pp.

Li, C., and P. Xian, 2003: Atmospheric anomalies related to interdecadal variability of SST in the North Pacific. *Adv. Atmos. Sci.,* **20,** 859–874.

Li, Q. X., X. Liu, H. Zhang, T. C. Peterson, and D. R. Easterling, 2004: Detecting and adjusting temporal inhomogeneity in Chinese mean surface air temperature data. *Adv. Atmos. Sci.,* **21,** 260–268.

Liu, B., M. Xu, M. Henderson, and W. Gong, 2004: A spatial analysis of pan evaporation trends in China, 1955–2000. *J. Geophys. Res.,* **109,** D15102, doi:10.1029/2004JD004511.

Liu, H. B., and X. M. Shao, 2003: A reconstruction of early spring mean temperature of history time over the Qinling Mountains. *Acta Geogr. Sin.,* **58,** 879–884.

Menon, S., J. Hansen, L. Nazarenko, and Y. Luo, 2002: Climate effects of black carbon aerosols in China and India. *Science,* **297,** 2250–2253.

Qian, W. H., D. L. Chen, Y. Zhu, and H. Y. Shen, 2003: Temporal and spatial variability of dryness–wetness in China during the last 530 years. *Theor. Appl. Climatol.,* **76,** 13–29.

——, ——, X. Lin, and A. M. Qin, 2004: Change trends of regional temperature and precipitation over China under background of global change. *Climate Change Newsletter,* No. 3, China IPCC Office and National Climate Center, Beijing, China, 8–9.

Qian, Y., D. P. Kaiser, L. R. Leung, and M. Xu, 2006: More frequent cloud-free sky and less surface solar radiation in China from 1955 to 2000. *Geophys. Res. Lett.,* **33,** L01812, doi:10.1029/2005GL024586.

Qin, D. H., Y. H. Ding, and J. L. Su, Eds., 2005: *Changes of Climate and Environment in China*. Vol. 1. Science Press, 562 pp.

Ren, G. Y., Ed., 2007: *Climate Change and Water Resources in China*. China Meteorological Press, 314 pp.

——, H. Wu, and Z. H. Chen, 2000: Spatial characteristics of precipitation change over China. *J. Appl. Meteor. Sci.,* **11,** 322–330.

——, J. Guo, M. Z. Xu, Z. Y. Chu, L. Zhang, X. K. Zou, Q. X. Li, and X. N. Liu, 2005: Climate changes of mainland China over the past half century. *Acta Meteor. Sin.,* **63,** 942–956.

——, Y. Q. Zhou, Z. Y. Chu, A. Y. Zhang, J. Guo, and X. F. Liu, 2008: Urbanization effects on observed surface air temperature trends in north China. *J. Climate,* **21,** 1333–1348.

Sandwell, D. T., 1987: Biharmonic spline interpolation of GEOS-3 and SEASAT altimeter data. *Geophys. Res. Lett.,* **14,** 139–142.

Solomon, S., D. Qin, M. Manning, M. Marquis, K. Averyt, M. M. B. Tignor, H. L. Miller Jr., and Z. Chen, Eds., 2007: *Climate Change 2007: The Physical Science Basis*. Cambridge University Press, 996 pp.

Tang, G. L., and G. Y. Ren, 2005: Reanalysis of surface air temperature change of the past 100 years over China. *Climate Environ. Res.,* **10,** 791–798.

Torrence, C., and G. P. Compo, 1998: A practical guide to wavelet analysis. *Bull. Amer. Meteor. Soc.,* **79,** 61–78.

Tu, Q. P., Z. W. Deng, and X. L. Zhou, 2000: Study on regional feature of China temperature variation. *Acta Meteor. Sin.,* **58,** 288–296.

von Storch, H., and F. W. Zwiers, 1999: *Statistical Analysis in Climate Research*. Cambridge University Press, 484 pp.

Wang, H. J., 2001: The weakening of the Asian monsoon circulation after the end of 1970's. *Adv. Atmos. Sci.,* **18,** 376–386.

Wang, S., and D. Gong, 2000: Enhancement of the warming trend in China. *Geophys. Res. Lett.,* **27,** 2581–2584.

——, ——, and J. Ye, 2000: Precipitation series and the variability of four seasons since 1880 over eastern China. *Acta Geogr. Sin.,* **55,** 281–293.

——, and Coauthors, 2005: Climate change of China. *China Climate and Environment Changes,* Q. Dahe, D. Yihui, and S. Jilan, Eds., Vol. 1, Science Press, 63–103.

Xu, C. Y., L. Gong, T. Jiang, D. Chen, and V. P. Singh, 2006: Analysis of spatial distribution and temporal trend of reference evapotranspiration and pan evaporation in Changjiang (Yangtze River) catchment. *J. Hydrol.,* **327,** 81–93.

Xu, Q. 2001: Abrupt change of the mid-summer climate in central east China by the influence of atmospheric pollution. *Atmos. Environ.,* **35,** 5029–5040.

Yan, Z., and Coauthors, 2002: Trends of extreme temperatures in Europe and China based on daily observations. *Climatic Change,* **53,** 355–392.

Zeng, Z., Z. Yan, and D. Ye, 2001: Regions of most significant temperature trend during the last century. *Adv. Atmos. Sci.,* **18,** 481–496.

Zhai, P. M., X. H. Pan, 2003: Trends in temperature extremes during 1951–1999 in China. *Geophys. Res. Lett.,* **30,** 1913, doi:10.1029/2003GL018004.

Zhang, D. E., 1988: Method of reconstructing the dryness-wetness series in China for the last 500 years and its reliability. *The Reconstruction of Climate in China for Historical Times,* J. C. Zhang, Ed., Science Press, 18–30.

——, X. Q. Li, and Y. Y. Liang, 2003: An extension of the yearly charts of dryness/wetness in China over the last 500 years. *J. Appl. Meteor. Sci.,* **14,** 379–388.

Zhang, J. C., and T. J. Crowley, 1989: Historical climate records in China and reconstruction of past climates. *J. Climate,* **2,** 833–849.

Zhao, Z. C., S. W. Wang, Y. Xu, G. Y. Ren, Y. Luo, and X. J. Gao, 2005: An analysis of possible causes of China surface air temperature change in the past 100 years. *Climate Environ. Res.,* **10,** 808–817.

Zheng, H., L. Zhang, C. Liu, Q. Shao, and F. Yoshihiro, 2007: Changes in stream flow regime in headwater catchments of the Yellow River basin since the 1950s. *Hydrol. Proc.,* **21,** 886–893, doi:10.1002/hyp.6280.

Zheng, J., W.-C. Wang, Q. Ge, Z. Man, and P. Zhang, 2006: Precipitation variability and extreme events in eastern China during the past 1500 years. *Terr. Atmos. Oceanic Sci.,* **17,** 579–592.

Zhou, L. T., and R. H. Huang, 2003: Research on the characteristics of interdecadal variability of summer climate in China and its possible cause. *Climatic Environ. Res.,* **8,** 274–290.